Exploring the mechanical response of low-carbon soil improvement mixtures

Alessandro Fraccica[1], Giovanni Spagnoli[2]*, Enrique Romero[1,3], Marcos Arroyo[1,3], Rodrigo Gómez[3]

[1] Geomechanics Group, International Centre for Numerical Methods in Engineering, Campus Nord UPC, calle Gran Capità, S/N 08034 Barcelona, Spain

[2] MBCC Group, Dr.-Albert-Frank-Straße 32, 83308 Trostberg, Germany, giovanni.spagnoli@mbcc-group.com, spagnoli_giovanni@yahoo.de, https://orcid.org/0000-0002-1866-4345 (corresponding author)

[3] Department of Civil and Environmental Engineering, Universitat Politècnica de Catalunya, calle Jordi Girona, 1-3, 08034 Barcelona, Spain

ABSTRACT

As society moves towards decarbonisation it is important to assess the hydro-mechanical behaviour of binders that could offer a low-carbon alternative to Portland cement in ground improvement technologies. This work considers two such alternatives: one still largely unexplored (metakaolin-based geopolymers) and a better known one (colloidal silica). Results from unconfined compressive strength, permeability tests, undrained monotonic and cyclic triaxial tests on granular soils (sand and silty sand) treated with those two binders are presented and discussed, emphasizing similitudes and differences with the response of similar soils treated with other conventional and unconventional binders. Effects of silt content, curing conditions and soil/binder ratios are examined. Both colloidal silica and metakaolin-based geopolymer significantly improve the mechanical properties of the treated soils, although the geopolymer results in a stronger and stiffer material. Both treatments reduce much the permeability of the treated soil, but the reduction achieved with CS is larger.

Keywords: sand-silt mixture; triaxial tests; permeability; metakaolin-based geopolymer; colloidal silica

ABBREVIATIONS AND SYMBOLS

C_{iv}	Volumetric cement content
D_r	Relative density
c’	Drained cohesion
e	Void ratio
E	Young modulus
F_0	Metakaolin volumetric filling
FA	Fly-ash
G_S	Specific gravity
k_w	Water permeability
MK	Metakaolin
OPC	Ordinary Portland cement
q	Deviatoric stress amplitude
TXCIU	Monotonic triaxial compression test
CTXU	Cyclic triaxial compression test
UCS	Unconfined compressive strength test
ρ_s	Density of the solid particles (components)
$\rho_s{}^*$	Density of the solid particles in the mixture
ϕ	Diameter

47	φ'	Drained friction angle
48	v	Poisson's ratio
49	η	Porosity

INTRODUCTION

Ground improvement techniques enhance the mechanical and hydraulic properties of soils for engineering applications. Several ground improvement methods involve the addition of binders to soils in place. These methods are usually classified according to the level of soil disturbance associated with binder placement (e.g., Cambefort, 1977; Mitchell, 1981; Karol, 2003; Spagnoli, 2021). Techniques based on mechanical mixing, such as deep soil mixing, or fluid-driven erosion and mixing, such as jet-grouting, require total soil remoulding and occupy one end of this spectrum. At the other end are located techniques that imply very low disturbance, such as permeation grouting. Regardless of the technology selected, the binder that is currently most often employed in ground improvement technology is ordinary Portland cement (OPC).

Cement manufacturing accounts for 8% of global carbon dioxide (CO_2) emissions and reducing the carbon dioxide footprint of concretes is increasingly seen as urgent (IEA, 2018). Low-carbon binders, in which OPC has been totally substituted, are key to achieve significant long-term emission reductions (Lehne and Preston, 2018). This fits well with the perception of material use as the dominant factor in life-cycle environmental impact of geotechnical systems (Kendall et al 2017). Referring particularly to ground improvement, life-cycle carbon emissions have been proposed as a means to evaluate the global environmental impact of specific projects (Shillaber et al. 2016). It is thus likely that the road towards sustainable ground improvement passes through a much-increased use of low-carbon binders (Mohammed et al. 2021).

Alkali-activated binders (AAB) represent one important low-carbon alternative to OPC (Provis and Deventer, 2014). AAB result from the reaction of a solid alumino-silicate based material (precursor) and an alkaline metal (activator, e.g. sodium hydroxide). A variety of products can act as precursors in AAB. Important examples include industrial

wastes, (such as ground blast-furnace slag (GBFS) or fly-ash residue from coal-fired electricity generation), as well as natural products, (such as volcanic ash or a calcined kaolinite known as metakaolin). The potential of AAB for ground improvement applications has been repeatedly highlighted from a variety of perspectives from strength improvement (e.g. Cristelo et al., 2011; Canakci et al. 2019) to environmental remediation (Ji and Pei, 2019; Du et al. 2020). Finally, it is worth noting that the use of AAB is not the only alternative to obtain low-carbon binders for ground improvement, as other residues (e.g. calcium carbide, Du et al. 2016) and additives (e.g. superphosphate, Xia et al. 2017, 2019) are also useful for that purpose.

Metakaolin (MK) and low-calcium fly-ash result in almost exclusively aluminosilicate AABs, which are generally known as geopolymers (Davidovits, 1994, 2008; Provis and Bernal, 2014). The term “geopolymer” describes an amorphous network of polymerized silicoaluminates (Ma et al. 2018). Geopolymers are also used in the concrete industry as full or partial replacement for conventional cements (e.g. Singh et al. 2015).

Metakaolin is an industrial product, generally having more consistent properties than residue-based AAB. The raw material (clay) is abundant (IEA, 2018) and, unlike some residues, will not be limited by foreseeable changes in technology (as is the case of GGBS) or in the energy production mix (as is the case of FA). On the other hand, the current production of metakaolin is still small and it is currently marketed at significantly higher prices per weight that OPC or other AAB precursors.

Metakaolin-based binders are highly viscous (Provis and Bernal, 2014). This makes them unsuitable for soil permeation purposes, and better adapted for techniques such

as deep-mixing. A low-carbon alternative to OPC for permeation purposes is colloidal silica (CS). Colloidal silica of interest in ground permeation takes the form of manufactured aqueous suspensions of nanometric silica particles, solidifying as gel at a rate controlled by pH and salt concentration (Bergna and Roberts, 2006). CS has several inherent advantages for permeation treatments, such as small particle size, low viscosity and non-toxicity. All these benefits have driven the uptake of CS for ground improvement in geo-environmental (Moridis et al. 1995; Wong et al. 2018) and liquefaction mitigation applications (Gallagher et al., 2007; Zhao et al., 2020). It turns out that CS treatments are also advantageous over OPC-alternatives from the carbon emission viewpoint (Gallagher et al. 2013)

As with any other geomaterial, good mechanical and hydraulic characterization of binder-soil mixtures is necessary to achieve sustainable design objectives, as the alternative is overdesign and/or increased failure risk (Basu et al. 2015). Hydromechanical characterization studies of soils improved with CS are well advanced (e.g., Persoff et al, 1998; Gallagher and Mitchell, 2002; Díaz-Rodríguez et al., 2008; Porcino et al., 2011; Porcino et al., 2012; Vranna and Tika, 2015; Georgiannou et al., 2017; Salvatore et al., 2020). Table 1 presents a brief summary of such work: one aspect that has not been investigated previously is the effect of fines on CS treatment.

Mechanical investigations of soil treated with metakaolin-based geopolymer are limited. Some studies (e.g. Kolovos et al., 2013; Cyr et al., 2013; Deng et al., 2015; Wu et al., 2016; Asteris et al., 2017) have assessed the use of metakaolin in soil treatment as a partial Portland substitute, but they used no alkali activators and, therefore, the resulting binders were not geopolymers. Furthermore, when metakaolin-based geopolymers have been used, mechanical testing was limited to unconfined compressive strength (Zhang et al. 2013; Rong-rong and Dong-dong, 2020; Spagnoli et al. 2021a).

The situation is different for residue-based geopolymer-soil mixtures where initial scoping studies (Verdolotti et al., 2008; Cristelo et al., 2013; Singhi et al., 2016; Yaghoubi et al., 2018) have been followed by more in-depth mechanical studies (Rios et al. 2016; 2017; Abdullah et al. 2019, 2020).

Spagnoli et al. (2021b) presented a detailed study of the effect of curing conditions on microstructural and hydraulic properties of metakaolin-soil mixtures. However, the mechanical response was only explored by means of unconfined compression tests. It is thus necessary to perform more in-depth studies of the mechanical response of metakaolin treated soils, for instance with triaxial tests where effective stress can be controlled and pore pressure is registered.

The purpose of this work is to partially fill that gap in the current knowledge and present a study of the monotonic and cyclic triaxial strength of soils (a sand and a silty sand) treated with a metakaolin-based geopolymer. For contrast, the results are presented alongside those obtained with a CS treatment of the same soils: this had the added interest of examining the effect of soil fines in the CS treatment, an aspect that was not touched upon in previous studies.

MATERIALS AND METHODS

Base materials

Two reference granular soils were used for the treatment. The first one is Holcim quartz sand (0.2-0.6mm). The second is silty sand obtained by mixing dry carbonate silt ($CaCO_3$) in a proportion of 10% by weight with the previous reference sand. The grain size distribution of the soils is presented in Figure 1. Chemical and physical properties of the materials, as well as their initial state, are summarized in Table 2.

147 The first binder employed in this study uses CS (MasterRoc MP 320®, Master Builders
148 Solutions) as precursor. This product is an aqueous dispersion (density 1.30 Mg/m3)
149 of silica particles of uniform nanometric size and silica concentration of 40% (Table 2).
150 The CS was mixed with a solution of NaCl (10% solution) at a volume ratio of 12% to
151 induce the gelation process.

152 For the geopolymer employed here the precursor material was a metakaolin powder
153 (Argical™-M 1000, Imerys) (Table 2), a dehydroxylated aluminium silicate
154 ($Al_2O3{\cdot}2SiO_2$) resulting from the calcination and micronization of kaolinitic clay and
155 having lamellar-shaped particles. The metakaolin powder was activated with an alka-
156 line water solution of potassium silicate ($w(SiO_2)/w(K_2O) = 1$). Potassium silicate was
157 selected to enhance workability, as it is known to result in less viscous binders than
158 the more frequently employed sodium-based activators (Provis and Bernal, 2014).

159

160 *Sample preparation*

161 The CS suspension was mixed with the accelerator saline solution (Table 3), stirred
162 for 1 minute (with a Robot 500, 500W (Taurus, Spain)) and permeated into the soils,
163 which had been previously dry poured in the moulds from a height of 200 mm. Perme-
164 ation took place through the porous steel base of the moulds, driven by an air-liquid
165 interface system applying an injection pressure of 3 kPa. Injection continued until the
166 injected fluid fully permeated the specimen, in a process that always lasted less than
167 5 minutes. Tomographic inspection of permeated specimens (Figure 2) showed that
168 the process resulted in a very uniform and complete filling of pore space by the hard-
169 ened colloid.

Equal weights of potassium silicate, de-aired water and metakaolin powder were mixed (refer to Table 3), obtaining a Si/Al ratio of 1.3 and a water/binder mass ratio of 2. This last ratio is analogous to the water/cement ratio used in deep mixing applications with OPC (e.g., Puppala et al., 2008; BAUER Maschinen GmbH, 2016). The slurry obtained was mechanically mixed (as described for CS) for 5 minutes to reach a homogeneous lump-free dispersion of density 1.37 Mg/m^3, and then hand-mixed with the soils with a spatula. The resulting binder-soil material was poured in the moulds from a height of 200 mm. The mould walls were then lightly hit with a rubber hammer to remove some entrapped air bubbles in the mixtures, until the target specimen height was attained.

Each specimen was left in the mould for one day. Afterwards two different curing protocols were followed. Dry curing (D) consisted on leaving specimens until testing at a room temperature of 20°C and relative humidity 50%. Wet curing (W), which was only used for some metakaolin specimens, involved submerging specimens in de-aired water at 20°C. Immersion started three days after the preparation when they displayed adequate consistency. Since tests were carried out after 3, 7 and 28 days of curing, there is no difference between W and D specimens at three days. Dry curing is considered more realistic for applications of deep soil mixing in unsaturated soil and/or in exposed conditions, such as retaining walls (Mosadegh et al.2017; Le Kouby et al. 2018).

The as-poured Holcim sand void ratio was e = 0.825, corresponding to a relative density D_r = 35% (refer to Table 2 for minimum and maximum void ratios of the sand). The addition of 10% by weight of carbonate silt in the sand resulted in an as-poured void ratio e = 0.584. The volume of geopolymer slurry added to the soil was selected to fill a fixed fraction F_0 of the as-poured soil porosity. Two different filling target ratios were selected, F_0 = 40 or 100% The weight ratios resulting from these two different filling

195 targets F_0 are indicated in Table 4. In the table, the volumetric cement content C_{iv},
196 representing the fraction of dry metakaolin powder volume in the total volume of the
197 specimens (Consoli et al. 2012), and the ratio between the as compacted/poured soil
198 porosity η and C_{iv} are also shown. The water content / ponderal binder content, defined
199 as indicated by Horpibulsuk et al. (2005) and Cai et al. (2015), has been included in
200 the Table 4, as well.

201 Specimens were fabricated at two different sizes: UC-size specimens (D = 70 mm; h
202 = 140 mm) for UCS, and TX-size specimens (D = 38 mm; h = 76 mm) for cyclic and
203 monotonic TX testing and hydraulic measurements. The ends of each specimen were
204 trimmed with a diamond band saw and then sanded before testing, to obtain smooth
205 faces and a height/diameter ratio equal to 2 (ASTM D4767, 2017; ASTM 2166, 2017).

206 An overview of the experimental program is summarized in Table 5. The following no-
207 menclature is used to identify different specimens. The first letters indicate the compo-
208 sition: MK: pure geopolymer, S: sand, SO: sand + carbonate silt, CS: colloidal silica,
209 SMK: sand + geopolymer, SOMK: sand + carbonate silt + geopolymer, SCS: sand +
210 colloidal silica, and SOCS: sand + carbonate silt + colloidal silica. The number in pa-
211 renthesis indicates the target initial filling ratio for the mixtures (F_0). The curing condi-
212 tions are indicated by W and D. Finally, numbers (1, 3, 7, 14, 28) indicated the elapsed
213 curing time in days before testing. For instance, a sample of sand treated with an initial
214 colloidal silica filling equal to 100% of the pore volume, tested after 28 days of curing
215 at 50% RH, would be SCS(100)D28.

216 *Hydraulic and mechanical tests*

Unconfined compressive strength tests (UCS) followed a standard procedure (ASTM 2166, 2017) which involved an axial-strain rate of around 0.5%/min (see Spagnoli et al. 2021a, for more detail).

Isotropically consolidated undrained triaxial compression tests (TXCIU) were carried out at isotropic consolidation pressures of p'_0 = 200 and 600 kPa. To ensure saturation during shearing, a back pressure of u_w = 500 kPa was applied and maintained for at least 24 hours before shearing. The undrained shearing stage was conducted under stress-controlled conditions (47 kPa/min). Secant Young moduli were calculated at different axial straining (ε_{ax} = 0.01% and 2.50%).

Permeability of TXCIU specimens was measured in the triaxial cell, at the beginning of each test. A controlled hydraulic gradient was applied using a back-pressure of 100 kPa at the bottom and of 10 kPa at the top cap. The inflow and outflow fluid volumes were recorded by pressure/volume controllers, and the saturated permeability was calculated under steady-state conditions (equal inflow and outflow fluid volume rates). An isotropic confining total stress of 200 kPa was imposed during the measurement.

Saturated TX-size specimens were also tested under cyclic triaxial undrained compression (CTXUC). Saturation was performed using a back-pressure of 400 kPa, while maintaining p' = 10 kPa. Subsequently, an anisotropic consolidation stage following a K_0 = 0.5 stress path was carried out until reaching radial and vertical effective stress $\sigma'_{3,aver}$= 125 kPa and $\sigma'_{1,aver}$ = 250 kPa, respectively. The consolidation stage lasted around 24 hours. Finally, 600 cycles at a frequency of 1 Hz were applied to the material under undrained conditions. The cycles were of pure compression with a cyclic stress ratio *CSR* = 0.25. This variable is defined as (Kramer, 1996):

$$CSR = \frac{q}{2\sigma'_0} \quad (1)$$

$$\sigma'_0 = \frac{1+2K_0}{3}\sigma'_{1,aver.} \quad (2)$$

where q is the deviatoric stress amplitude, $\sigma_1 - \sigma_3$, and σ'_0 is the mean effective confining stress.

Secant undrained moduli were obtained for all cycles. These were computed on the backbone q-ε_{ax} curve of each cycle (Matasovic and Vucetic, 1993; Subramaniam et al. 2019).

RESULTS

Unconfined compressive strength (UCS)

Axial stress-strain curves for different UCS tests are presented in Figure 3. For similar curing conditions geopolymer treated soils showed order of magnitude higher strengths than those injected with colloidal silica. This may be related to the strength of the two binders, which is generally much larger for the metakaolin geopolymer. For instance, for wet curing at 28 days Spagnoli et al (2021a) report UCS values of 1.2 MPa for specimens of pure MK, whereas Axelsson (2006) has reported values of only 40 kPa for a 35% CS gel cured in similar conditions.

The effect of curing is also different for the two treatments. It has been reported that dry curing of pure CS results in even higher strength gains than wet curing (Axelsson, 2006). On the other hand, dry curing of pure MK results in severe mechanical damage to the material (Spagnoli et al. 2021a). This was borne out by our tests, where in dry-cured CS treated specimens UCS systematically increased, whereas metakaolin treated specimens (SMK(100)D and SOMK(100)D) reduced strength and became more ductile during the curing period. The MK mixtures achieve higher strengths at all the curing times when cured below water (compare panel A and B in Figure 3).

Despite those differences, there are also some commonalities in the UCS strength of the mixtures resulting from the two different treatments. To begin with it is noteworthy that the mixtures are, in both cases, stronger than their component materials. It is also interesting to observe that, both for the CS and the MK geopolymer treatment, the presence of some silt within the sand results in stronger materials; the beneficial effect of a carbonate filler in dry-cured mixes has also been observed in OPC-based concrete (Bonavetti et al. 2000)

There are many factors that affect the UCS of treated soil specimens. Consoli and co-workers (2011; 2012; 2016; 2020) have advocated the use of the porosity/binder ratio η/C_{iv} as a normalizing factor accounting for void ratio of the host soil (through the dry mix porosity value, η) and binder dosage (through the volumetric ratio, C_{iv}). Figure 4 (a) uses this parameter to compare the strength performance of the materials tested in this study with some previous work. The comparison indicates that the treatment with MK-based binder results in mechanical performance similar to those of OPC-based treatments. At the same porosity / binder ratio CS treatments result in materials that are significantly weaker than those treated with either OPC or geopolymer, and better aligned with unconventional treatments such as the waste-glass-carbide lime.

The UCS results are again presented in Figure 4 (b) using a different mixture ratio, namely the water content to ponderal binder dosage ratio, w/c_0, which is frequently used to interpret results of treated fine grained soils (Horpibulsuk et al. 2005; Cai et al. 2015). Interestingly, the results of both MK and CS treatments appear now better aligned with the trends from OPC. This result suggests that the much higher strength attained by MK treatments can be interpreted as a by-product of it being a relatively “dry” treatment, whereas CS is instead a very “wet” binder.

289 *Permeability*

290 Figure 5 shows the values of saturated water permeability calculated during the satu-
291 ration stage of the TXC tests. Permeation with CS reduced the permeability of the base
292 soils much more than mixing with the geopolymer slurry, even when that mix was de-
293 signed to fill all the voids in the soil. The higher impermeabilizing efficiency of the col-
294 loidal silica treatment is made clearer by plotting the permeability values against the
295 “as-cured” void ratio of the specimens (Figure 5b). At the same void ratio, the CS treat-
296 ment reduced soil permeability by one order of magnitude more than the geopolymer.
297 Note that “as-cured” void ratio was evaluated by the paraffin method and corroborated
298 with CAT image analysis, (see Table 6 and Spagnoli et al. 2021a for more detail).

299 A plausible explanation for this difference is given by the different microstructural fea-
300 tures of the binders, as observed by microscopy (SEM and FESEM). While the me-
301 takaolin geopolymer results in micron-scale heterogeneity (Kuenzel et al. 2012; Katsiki
302 et al.2019; Spagnoli et al. 2021a) the microstructure of CS is only heterogenous at the
303 nanoscale and has smaller pores than those present in the geopolymer (Wong et al.
304 2018, Porcino et al. 2011).

305 *Monotonic triaxial undrained compression (TXCIU)*

306 The deviatoric stress and the excess pore water pressure observed during the shear-
307 ing stage of the CU triaxial tests are presented in Figure 6 and Figure 7.

308 At the same target filling ratio sand specimens improved with geopolymer are stronger,
309 dilate more and are stiffer than those improved with CS. They also have a more brittle
310 failure. The same conclusions can be drawn from the results obtained on silty sand.
311 Dilatancy reduces at the higher confining stress (p'_0 = 600 kPa) for all materials. In-

creasing the filling ratio for geopolymer resulted in more dilatant and stronger specimens. Similar trends were observed by Wong et al. (2018) and Georgiannou et al. (2017) in CS-treated soils.

Contrary to what happened with UCS the effect of curing time on the triaxial response of dry-cured MK treated specimens was rather small, showing lesser or no clear decay of peak mobilised strength with time (Figure 8). This suggests that confinement inhibited the mechanical effect of MK micro-cracking that was visible on microscopic images (Spagnoli et al. 2021a)

Undrained secant Young moduli are presented in Figure 9 (at a small strain level) and Figure 10 (at intermediate strain levels). In these figures the strain level effect (decreasing stiffness as strain level increases) is larger than the stress level effect (stiffness increases as confinement increases). As for the time effect, there is little to no evidence of stiffness reduction due to dry-curing on the geopolymer-soil mixtures. On the contrary, a certain curing-induced increase of stiffness at both strain levels is visible, although more for the silty sand (SO) based mixtures than for the pure sand (S) mixtures. For the CS treated specimens the increase of stiffness with curing is even more consistent.

Cyclic triaxial undrained compressions (CTXUC)

The evolution of normalized excess pore pressure during cyclic loading is shown in Figure 11, along the axial strain and the number of cycles. The normalizing stress employed is the minor principal effective stress at consolidation, as is customary for triaxial conditions. The untreated specimens S and SO underwent high strains (i.e. $\varepsilon_{ax} >$ 5%) within the first 10 cycles of loading already, jointly with a fast increase of the pore water pressures. They reached values of r_u between 0.7 (clean sand) and 0.85 (sand

336 + fines), which are close to a condition of liquefaction of the material. This might reflect
337 an increased relative density in the silty sand (Polito and Martin, 2003) although it is
338 recognized that the effect of non-plastic fines on liquefaction is a complex issue, be-
339 yond the scope of this paper.

340 In all the treated samples the effect of the applied cycles was not dramatic and axial
341 strains remained lower than 1%. Soils treated with CS showed higher strains and ex-
342 cess pore water pressures than those treated with the metakaolin geopolymer. This
343 may be attributed to the combined effect of smaller stiffness and lower permeability of
344 the CS treatment.

345 The stress path of the treated specimens remains distant from the triaxial failure enve-
346 lope (Figure 12). Notwithstanding that, significant stiffness degradation took place dur-
347 ing cyclic loading, even for the stronger MK treated material. In Figure 13, the effect of
348 cycling on the normalized secant undrained Young modulus $E_u/E_{u,in.}$ is presented along
349 the cycles. $E_{u,in.}$ is the stiffness calculated on each CTXUC backbone curve, in corre-
350 spondence of the first shearing cycle. The final secant stiffness is around 5 MPa (2%
351 of $E_{u,in.}$) in the untreated samples, 55 MPa (13% of $E_{u,in.}$) in CS-treated samples, and
352 236 MPa (43% of $E_{u,in.}$) in MK-treated samples.

353 **DISCUSSION**

354 As pointed out before precursor materials for geopolymers not only include metakaolin
355 but also low calcium fly ash. Rios et al. (2016, 2017, 2017b) presented a mechanical
356 study of silty sand treated with a fly ash based geopolymer. The base materials were
357 similar to those employed here (see Figure 1). The binder dosage in the mixtures was
358 slightly higher and the porosity was slightly lower (see Table 7).

Figure 14 and Figure 15 compare the peak strength envelopes obtained with the different base soils alone and with the geopolymer treated soils, (see also Table 8). Note that in the triaxial tests by Rios et al. (2017) the specimens were sheared in a drained condition, after anisotropic consolidation, whereas here shearing is undrained and consolidation isotropic. Despite those differences, the two sets of results fit well together. The envelopes obtained for the base soils are remarkably close, a fact that allows better appreciation of the relative improvement obtained by each binder mixture. The strength attained increases as the MK dosage increases and also when silt is added to the sand. This last effect may be due to the silt reducing the soil porosity, although a chemical effect -the strengthening of geopolymer by small doses of calcium carbonate (Yip et al. 2008)- may also play a role. The FA treatment results in higher envelopes which, again, may be first related to the smaller porosity/binder ratio (Table 7) and perhaps also to the different binder chemistry.

Secant stiffness degradation during shearing, $E_u/E_{u,0.01}$, is compared in Figure 16 for the different geopolymer improved soils. $E_{u,0.01.}$ is calculated in correspondence of an axial strain of 0.01%, as for Figure 9. The results suggest that the MK geopolymer and CS are somewhat more fragile than the FA one, as the stiffness decay is faster. Again, the effects of dosage and porosity may explain the difference, although other factors may also play a role. One such factor is the harsher curing condition of the MK specimens, where dry curing resulted in visible retraction microcracks in the binder joining together the different grains (Figure 19).

By comparison with the geopolymers, the strength increase obtained with the CS treatment is much smaller (Figure 17). The results are in good agreement with direct shear results obtained by Wong et al. (2018) on a CS treated sand similar to the one in this study (MP 320, silica concentration = 40% (w/w) in the solution). The limited effect of

CS on friction angle was also observed by Wong et al. (2018) and Vranna and Tika (2015). It is noticeable that, contrary to what happened for the UCS, the addition of carbonate silt did not induce significant effects on the triaxial envelope of the CS improved soil.

The permeability values obtained in this work are compared with similar measurements in Figure 18. The important role of the curing condition on this property is evidenced by the results for CS which was more permeable when cured dry, even for relatively more intense binder treatment (as measured by the w/c_0 ratio).

The observed differences between CS and MK treated soils can be related to some features of the induced microstructure. Both binders fill in the gaps between the soil grains, cementing them. But the metakaolin geopolymer presents pervasive retraction cracking at the microscale (Figure 19; see also Spagnoli et al. 2021a), whereas the CS cement bridges, with nanoscale porosity, have a much smoother texture (see Wong et al. 2018).

CONCLUSIONS

This paper investigated the influence of two different binders (i.e. metakaolin-based geopolymer and colloidal silica) on the hydro-mechanical behaviour of loose sandy soils under monotonic and cyclic stresses. The main observations may be summarized as follows

- Treatment with metakaolin-based geopolymer is as effective to increase the strength of the soils as OPC, attaining similar UCS values for similar porosity/binder ratio values
- Although dry-curing reduces the UCS of metakaolin treated soil, it did not reduce its confined (triaxial) strength or stiffness,

- The strength improvements obtained with the metakaolin geopolymer and the colloidal silica are generally well aligned with those obtained with Portland Cement at similar w/c_0 dosage ratios.
- Metakaolin treated soils had larger stiffness and slower stiffness degradation than those permeated with CS
- Although both treatments achieved significant reductions in permeability, treatment with CS was more effective to reduce permeability than treatment with the metakaolin geopolymer.
- Both treatments improved significantly the cyclic response of the sandy soils, within the number of cycles investigated, exhibiting low pore-water pressures and axial strains.
- The presence of carbonate silt within geopolymer-treated specimens resulted in a slight increase of soil cohesion and stiffness, while negligible effects were observed in CS-treated samples.
- Finally, the mechanical improvement obtained with the metakaolin-based geopolymer is well aligned with previous observations on fly-ash based geopolymers.

The dominant role of OPC in ground improvement technologies results from various important factors, including a well proven track record, economic considerations and technical familiarity. Systematic and extensive geomechanical studies of low-carbon alternatives are required for this situation to change. Given the large strength increases obtained in this work, future work on the mechanical and hydraulic properties of metakaolin-based geopolymers should explore the possibility of using smaller binder dosages. The complexities added by realistic curing scenarios must also continue to be explored, for instance addressing also the possible effect of curing under stress. Finally, laboratory testing should be complemented by field testing and demonstration projects of MK-based ground treatment.

ACKNOWLEDGEMENT

The authors wish to thank Master Builders Solutions for the permission granted to publish these results.

REFERENCES

Abdullah H.H., Shahin M.A., and Walske M.L. (2019) Geo-mechanical behaviour of clay soils stabilized at ambient temperature with fly-ash geopolymer-incorporated granulated slag. Soils and Foundation 59, 1906-1920

Abdullah H.H., Shahin M.A., Walske M.L., and Karrech A. (2020b) Cyclic Behaviour of Clay Stabilised with Fly-ash Based Geopolymer Incorporating Ground Granulated Slag. Transportation Geotechnics (In Press)

ASTM (2017) Volume 04.08 Soil and Rock (I): D420 – D5876/D5876M. West Conshohocken, PA, 19428-2959 USA.

Axelsson, M. (2006). Mechanical tests on a new non-cementitious grout, silica sol: A laboratory study of the material characteristics. *Tunnelling and Underground Space Technology*, *21*(5), 554-560.

Basu, D., Misra, A., and Puppala, A. J. (2015). Sustainability and geotechnical engineering: perspectives and review. *Canadian Geotechnical Journal*, *52*(1), 96-113.

BAUER Maschinen GmbH (2016). CSM-Cutter Soil Mixing. https://www.bauer.de/export/shared/documents/pdf/bma/datenblatter/CSM_Cutter_Soil_Mixing_EN_905_656_2.pdf905-656-2_EN.pdf (last accessed December 8, 2020)

Bergna, H. E., and Roberts, W. O. (Eds.). (2005). *Colloidal silica: fundamentals and applications* (Vol. 131). CRC Press.

Bonavetti, V., Donza, H., Rahhal, V., and Irassar, E. (2000). Influence of initial curing on the properties of concrete containing limestone blended cement. *Cement and Concrete Research*, *30*(5), 703-708.

Cai, G. H., Du, Y. J., Liu, S. Y., & Singh, D. N. (2015). Physical properties, electrical resistivity, and strength characteristics of carbonated silty soil admixed with reactive magnesia. Canadian Geotechnical Journal, 52(11), 1699-1713.

Cambefort, H. (1977). The principles and applications of grouting. Quarterly Journal of Engineering Geology and Hydrogeology, 10, 57-95, https://doi.org/10.1144/GSL.QJEG.1977.010.02.01.

Canakci, H., Güllü, H., and Alhashemy, A. (2019) Performances of Using Geopolymers Made with Various Stabilizers for Deep Mixing. Materials, 12, 2542

Cyr, M., Trinh, M., Husson, B., Casaux-Ginestet, G. (2013) Design of eco-efficient grouts intended for soil nailing. Construction and Building Materials 41, 857–867

Consoli, N. C., Cruz, R. C., and Floss, M. F. (2011). Variables controlling strength of artificially cemented sand: influence of curing time. Journal of Materials in Civil Engineering, 23(5), 692-696.

Consoli, N.C., da Fonseca, A.V., Silva, S.R., Cruz, R.C. and Fonini, A. (2012). Parameters controlling stiffness and strength of artificially cemented soils. Geotechnique 62(2), 177–183, http://dx.doi.org/10.1680/geot.8.P.084.

Consoli, N. C., Ferreira, P. M. V., Tang, C. S., Marques, S. F. V., Festugato, L. and Corte, M. B. (2016). A unique relationship determining strength of silty/clayey soils – Portland cement mixes. Soils and Foundations 56(6), 1082–1088.

Consoli, N.C., Da Silva Carretta, M., Festugato, L., Batista Leon, H., Ferreira Tomasi, L. and Salvagni Heineck, K. (2020) Ground waste glass–carbide lime as a sustainable binder stabilising three different silica sands. Géotechnique (Ahead of Print)

Cristelo, N., Glendinning, S. and Pinto, A. T. (2011). Deep soft soil improvement by alkaline activation. Proceedings of the ICE-Ground Improvement, 164, (2), 73–82.

Cristelo, N., Glendinning, S., Fernandes, L. and Pinto, A.T. (2013) Effects of alkaline-activated fly ash and Portland cement on soft soil stabilisation. Acta Geotechnica 8, 395–405. https://doi.org/10.1007/s11440-012-0200-9

Davidovits, J. (1994). Properties of geopolymer cements. 1st International Conference on Alkaline Cements and Concretes. Kiev, Ukraine: Kiev State Technical University, 131-149.

Davidovits, J. (2008). Geopolymer Chemistry and Applications. In: Saint Quentin, F.G.I. (Ed.).

Díaz-Rodríguez, J.A.; Antonio-Izarraras, V.M.; Bandini, P.; López-Molina, J.A. (2008) Cyclic strength of a natural liquefiable sand stabilized with colloidal silica grout. Canadian Geotechnical Journal, 45, 1345–1355. doi:10.1139/T08-072

Deng, Y., Yue, X., Liu, S., Chen, Y., Dingwen, Z. (2015) Hydraulic conductivity of cement-stabilized marine clay with metakaolin and its correlation with pore size distribution. Engineering Geology 193, 146-152

Dong, C., Zhang, R., Zheng, J., and Jiang, W. (2020) Strength behavior of dredged mud slurry treated jointly by cement, metakaolin and flocculant. Applied Clay Science 193, 105676

501 Du, Y.J., Jiang, N.J., Liu, S.Y., Horpibulsuk, S., and Arulrajah, (2016) Field evaluation
502 of soft highway subgrade soil stabilized with calcium carbide residue. Soils and Foun-
503 dations, 56(2), 301-314, https://doi.org/10.1016/j.sandf.2016.02.012

504 Du, Y.J., Wu, J., Bo, Y.L. and Jiang, N.J. (2020) Effects of acid rain on physical, me-
505 chanical and chemical properties of GGBS–MgO-solidified/stabilized Pb-contaminated
506 clayey soil. Acta Geotechnica, 15, 923–932, https://doi.org/10.1007/s11440-019-
507 00793-y

508 Ghadir, P., and Ranjbar, N. (2018) Clayey soil stabilisation using geopolymer and Port-
509 land cement. Construction and Building Materials, 188, 361-371.

510 Gallagher, P.M. and Mitchell, J.K. (2002). Influence of colloidal silica grout on liquefac-
511 tion potential and cyclic undrained behavior of loose sand. Soil Dynamics and Earth-
512 quake Engineering, 22, 1017–1026.

513 Gallagher, P.M., Pamuk, A. and Abdoun, T. (2007). Stabilization of liquefiable soils
514 using colloidal silica grout. Journal of Materials in Civil Engineering, 19(1), 33-40,
515 https://doi.org/10.1061/(ASCE)0899-1561(2007)19:1(33).

516 Georgiannou V.N., Pavlopoulou E.M., Bikos Z., (2017). Mechanical behaviour of sand
517 stabilised with colloidal silica. Geotechnical Research, 4(1), 1-11

518 International Energy Agency (2018) Technology Roadmap: Low-Carbon Transition in
519 the Cement Industry, IEA

520 Horpibulsuk, S., Miura, N., & Nagaraj, T. S. (2005). Clay–water⁄cement ratio identity
521 for cement admixed soft clays. Journal of geotechnical and geoenvironmental engi-
522 neering, 131(2), 187-192.

Ishihara, K., Yamazaki, A., Haga, K. (1985). Liquefaction of K0-consolidated sand under cyclic rotation of principal stress direction with lateral constrains. Soils and Foundations, 25(4), 63-74.

Ji Z., and Pei, Y. (2019). Bibliographic and visualized analysis of geopolymer research and its application in heavy metal immobilization: a review. Journal of Environmental Management 231, 256-267. https://doi.org/10.1016/j.jenvman.2018.10.041

Karol, R.H. (2003). Chemical Grouting and Soil Stabilization. Marcel Dekker, Inc., New York, NY.

Littlejohn GS (1993). Underpinning by chemical grouting. In Underpinning and Retention (Thorburn S and Littlejohn GS (eds)). Springer, New York, 242-275.

Lehne, J. and Preston, F. (2018). Making concrete change. London, UK: The Royal Institute of International Affairs.

Katsiki, A., Hertel, T., Tysmans, T., Pontikes, Y., and Rahier, H. (2019) Metakaolinite Phosphate Cementitious Matrix: Inorganic Polymer Obtained by Acidic Activation. Materials 12, 442

Kendall, A., Raymond, A. J., Tipton, J., and DeJong, J. T. (2017). Review of life-cycle-based environmental assessments of geotechnical systems. In *Proceedings of the Institution of Civil Engineers-Engineering Sustainability* (Vol. 171, No. 2, pp. 57-67). Thomas Telford Ltd.

Kolovos, K.G., Asteris, P.G., Cotsovos, D.M., Badogiannis E., and Tsivilis, S. (2013). Mechanical properties of soilcrete mixtures modified with metakaolin. Construction and Building Materials 47, 1026–1036.

545 Kramer, S. L. (1996). Geotechnical earthquake engineering. Prentice-Hall Civil Engi-
546 neering and Engineering Mechanics Series.

547 Kuenzel, C., Vandeperre, L.J., Donatello, S., Boccaccini, A.R., and Cheeseman C.
548 (2012) Ambient Temperature Drying Shrinkage and Cracking in Metakaolin-Based Ge-
549 opolymers. J. Am. Ceram. Soc., 95(10), 3270-3277

550 Le Kouby, A., Guimond-Barrett, A., Reiffsteck, P. & Pantet, A. (2018). Influence of dry-
551 ing on the stiffness and strength of cement-stabilized soils. Geotech. Geol. Engng 36,
552 No. 3, 1463–1474.

553 Ma, C.K., Awang, A.Z. and Omar, W. (2018) Structural and material performance of
554 geopolymer concrete: a review. Construction and Building Materials, 186, 90-102,
555 https://doi.org/10.1016/j.conbuildmat.2018.07.111

556 Matasovic, N., and M. Vucetic. 1993. “Cyclic characterization of liquefiable sands.”
557 Journal of Geotechnical Engineering. 119 (11), 1805–1822.
558 https://doi.org/10.1061/(ASCE)0733-9410(1993)119:11(1805).

559 Mitchell, J.K. (1981). Soil improvement-state of the art report. Proc. 10th ICSMFE, 4,
560 509-565.

561 Mohammed, M. A., Yunus, N. Z. M., Hezmi, M. A., Hasbollah, D. Z. A., and Rashid, A.
562 S. A. (2021). Ground improvement and its role in carbon dioxide reduction: a review.
563 Environmental Science and Pollution Research, 1-21.

564 Moridis,G.J.; Persoff., P.; Apps, J.A.; Myer, L.; Pruess, K.; Yen, P. (1995) A Field Test
565 of Permeation Grouting in Heterogeneous Soils Using a New Generation of Barrier
566 Liquids; Lawrence Berkeley Lab.: Berkeley, CA, USA.

567 Mosadegh, A., Szymkiewicz, F. & Nikraz, H. (2017). An experimental investigation of
568 the impact of specimen preparation and curing conditions on cement-treated material
569 strength (deep mixing method). Aust. J. Civ. Engng 15, No. 1, 49–60.

570 Murmu, A.L., Jain, A. and Patel, A. (2019) Mechanical properties of alkali activated fly
571 ash geopolymer stabilized expansive clay. KSCE Journal of Civil Engineering, 23(9),
572 3875-3888, DOI 10.1007/s12205-019-2251-z.

573 Persoff P, Apps J, Moridis G and Whang JM (1999). Effect of dilution and contaminants
574 of sand grouted with colloidal silica. Journal of Geotechnical and Geoenvironmental
575 Engineering, 125(6): 461-469.

576 Provis, J. L. and Bernal, S. A. (2014). Geopolymers and related alkali-activated mate-
577 rials. Annu. Rev. Mater. Res. 44, 299–327, https://doi.org/10.1146/annurev-matsci-
578 070813-113515.

579 Polito, C. P., and Martin, J. R. (2003). A reconciliation of the effects of non-plastic fines
580 on the liquefaction resistance of sands reported in the literature. *Earthquake Spectra*,
581 *19*(3), 635-651.

582 Porcino D, Marcianò V and Granata R (2011) Undrained cyclic response of a silicate-
583 grouted sand for liquefaction mitigation purposes. Geomechanics and Geoengineer-
584 ing: an International Journal 6(3), 155–170,
585 http://dx.doi.org/10.1080/17486025.2011.560287.

586 Porcino D, Marcianò V and Granata R (2012) Static and dynamic properties of a lightly
587 cemented silicate-grouted sand. Canadian Geotechnical Journal 49(10), 1117–1133,
588 http://dx.doi.org/10.1139/T2012-069.

589 Puppala, A.J., Madhyannapu, R.S., and Nazarian, S. (2008). Special Specification for
590 Deep Soil Mixing. Product 0-5179-P1, Project 0-5179, The University of Texas at Ar-
591 lington, Texas.

592 Rios, S., Cristelo, N., Viana Da Fonseca, A. and Ferreira, C. (2016). Structural perfor-
593 mance of alkali-activated soil ash versus soil cement. Journal of Materials in Civil En-
594 gineering, 28(2), 04015125 https://doi.org/10.1061/(ASCE)MT.1943-5533.0001398

595 Rios, S., Ramos, C., Viana Da Fonseca, A., Cruz, N., and Rodrigues, C. (2017). Me-
596 chanical and durability properties of a soil stabilized with an alkali-activated cement.
597 European Journal of Environmental and Civil Engineering, 23(2), 245-267.

598 Rios, S., Cristelo,N., Viana da Fonseca, A., and Ferreira, C. (2017b). Stiffness Behav-
599 ior of Soil Stabilized with Alkali-Activated Fly Ash from Small to Large Strains. Interna-
600 tional Journal of Geomechanics, 17(3), 04016087.

601 Rodrigues, P. M., Rodrigues, C., Cruz, N., Rios, S., & Viana da Fonseca, A. (2018).
602 Seepage water quality of a soil treated with alkali-activated cement at room tempera-
603 ture. Environmental Geotechnics, 6(7), 471-479. doi: 10.1680/jenge.17.00039

604 Romero, E., Gens, A. and Lloret, A. (1999) 'Water permeability, water retention and
605 microstructure of unsaturated compacted Boom clay', Eng. Geol. 54, 117–27

606 Romero, E., and Vaunat, J. (2000) 'Retention curves of deformable clays', in A. Tar-
607 antino and C. Mancuso (eds), International Workshop on Unsaturated Soils: Experi-
608 mental Evidence and Theoretical Approaches in Unsaturated Soils 91–106

609 Salvatore, E., Modoni, G., Mascolo, M.C., Grassi, D. and Spagnoli, G. (2020). Experi-
610 mental evidences on the effectiveness and applicability of colloidal nanosilica grouting

611 for liquefaction mitigation. Journal of Geotechnical and Geoenvironmental Engineer-
612 ing, 146,10, 04020108, DOI: 10.1061/(ASCE)GT.1943-5606.0002346.

613 Shillaber, C. M., Mitchell, J. K., and Dove, J. E. (2016). Energy and carbon assessment
614 of ground improvement works. I: Definitions and background. *Journal of Geotechnical*
615 *and Geoenvironmental Engineering*, *142*(3), 04015083.

616 Singh, B., Ishwarya, G., Gupta, M., and Bhattacharyya, S.K. (2015) Geopolymer con-
617 crete: A review of some recent developments. Construction and Building Materials, 85,
618 15, 78-90, https://doi.org/10.1016/j.conbuildmat.2015.03.036

619 Singhi, B., Laskar, A.I., and Ali Ahmed, M. (2016) Investigation on soil–geopolymer
620 with slag, fly ash and their blending. Arabian Journal for Science and Engineering 41,
621 393–400, DOI 10.1007/s13369-015-1677-y.

622 Spagnoli, G. (2021). A review of soil improvement with non-conventional grouts. Inter-
623 national Journal of Geotechnical Engineering, 15, 3, 273-287,
624 https://doi.org/10.1080/19386362.2018.1484603

625 Spagnoli, G., Romero E., Fraccica, A., Arroyo, M., and Gómez, R. (2021a) The effect
626 of curing conditions on the hydro-mechanical properties of a metakaolin-based soil-
627 crete. Géotechnique, https://doi.org/10.1680/jgeot.20.P.259

628 Spagnoli, G., Seidl, W., Romero, E., Arroyo, M., Gómez, R., and López J. (2021b).
629 Unconfined compression strength of sand-fines mixtures treated with chemical grouts.
630 Geotechnical Aspects of Underground Construction in Soft Ground, Elshafie, Viggiani,
631 Mair (eds.), CRC Press, Boca Raton, 829-835, DOI: 10.1201/9780429321559-109.

632 Subramaniam P., Banerjee S., and Ku T. (2019) Shear Modulus and Damping Ratio
633 Model for Cement Treated Clay. International Journal of Geomechanics (ASCE). 19,
634 7, 06019010

635 Verdolotti, L., Iannace, S., Lavorgna, M. and Lamanna R (2008). Geopolymerization
636 reaction to consolidate incoherent pozzolanic soil. Journal of Materials *Science* 43,
637 865–873. https://doi.org/10.1007/s10853-007-2201-x

638 Vranna A.D. and Tika T. (2015). The mechanical behaviour of a clean sand stabilized
639 with colloidal silica. Proceedings of the XVI ECSMGE Geotechnical Engineering for
640 Infrastructure and Development, Edinburgh (UK). ICE Publishing

641 Wichtmann, T., and Triantafyllidis, T. (2004). Influence of a cyclic and dynamic loading
642 history on dynamic properties of dry sand, Part i: cyclic and dynamic torsional pre-
643 straining. Soil Dynamics and Earthquake Engineering, 24(2):127–147.

644 Wong C., Pedrotti M., El Mountassir G., Lunn R.J. (2018) A study on the mechanical
645 interaction between soil and colloidal silica gel for ground improvement. Engineering
646 Geology 243, 84-100

647 Xia, W. Y., Feng, Y. S., Jin, F., Zhang, L. M., & Du, Y. J. (2017). Stabilization and
648 solidification of a heavy metal contaminated site soil using a hydroxyapatite based
649 binder. Construction and Building Materials, 156, 199-207.

650 Xia, W.Y., Du, Y.J., Li, F.S., Li, C.P., Yan, X.L., Arulrajah, A., Wang, F. and Song, D.J.
651 (2019) In-situ solidification/stabilization of heavy metals contaminated site soil using a
652 dry jet mixing method and new hydroxyapatite based binder. Journal of Hazardous
653 Materials, 369, 353-361, https://doi.org/10.1016/j.jhazmat.2019.02.031

654 Yaghoubi M, Arulrajah A, Disfani M.M., Horpibulsuk S., Bo M.W., Darmawan S. (2018)
655 Effects of industrial by-product based geopolymers on the strength development of a
656 soft soil. Soils and Foundations 58, 716-728

657 Zhang, M., Guo, H., El-Korchi, T., Zhang, G., and Tao, M. (2013) Experimental feasi-
658 bility study of geopolymer as the next-generation soil stabiliser. Construction and Build-
659 ing Materials 47, 1468–1478.

660 Zhao M., Liu G., Zhang C., Guo W., and Luo Q. (2020). State-of-the-Art of Colloidal
661 Silica-Based Soil Liquefaction Mitigation: An Emerging Technique for Ground Improve-
662 ment. *Appl. Sci.*, *10*(1), https://doi.org/10.3390/app10010015

663

TABLES

Table 1: Summary of previous geotechnical characterization studies on CS.

Year	Authors	CS	Mixture porosity, η *	CS concentration, C_{CS}, w/w (%)	silica/ dry soil w/w (%)	C_{iv}	Soil	Sample forming	Mech tests
1999	Persoff et al., 1999	DuPont Ludox SM	0.38	5 to 27	1.4 to 7.5	0.008 to 0.047	sand	Pluviation on grout	UCS
2002	Gallagher and Mitchell, 2002	DuPont Ludox SM30	0.429	5 to 20	1.7 to 6.8	0.010 to 0.039	loose sand	Pluviation on grout	UCS CTX
2008	Diaz Rodriguez et al. 2008	n.a.	0.482 to 0.502	14.5	6.8 to 7.4	0.036 to 0.037	fine sand	Pluviation on grout	K_0-cyclic simple shear
2011	Porcino et al., 2011	n.a.	0.417	10	2.9	0.017	sand	Permeation from base (3 pore volumes)	UCS Direct simple shear CSSU CTXU
2012	Porcino et al., 2012	TSG	0.417	10	2.9	0.017	sand	Permeation from base	TXCID cyclic simple shear

Year	Authors	CS	Mixture porosity, η *	CS concentration, C_{CS}, w/w (%)	silica/ dry soil w/w (%)	C_{iv}	Soil	Sample forming	Mech tests
2015	Vranna and Tika, 2015	Ludox SM30	0.408 to 0.432	10	3.1 to 3.5	0.019 to 0.020	sand	Permeation from base (4 specimen volumes)	TXCIU CTXCIU
2017	Georgiannou et al., 2017	Ludox SM30	0.355 to 0.432	10	2.5 to 3.5	0.016 to 0.020	sand	Pluviation on grout	UCS Direct shear test TXCID TXCAD
2018	Wong et al. 2018	MasterRoc MP 320	0.350 sand 0.480 kaolin	40	sand @ 11.7 % kaolin @ 61.7 %	sand @ 0.076 kaolin @ 0.321	Sand / Kaolin	Pouring CS on sand Hand mixing kaolin	Direct shear test Oedometer test

Year	Authors	CS	Mixture porosity, η *	CS concentration, C_{CS}, w/w (%)	silica/ dry soil w/w (%)	C_{iv}	Soil	Sample forming	Mech tests
2020	Ciardi et al., 2020	MasterRoc MP 325	0.405	2 to 13	0.6 to 3.7	0.003 to 0.022	sand	Pluviation on grout	Direct shear test Oedometer test CTXU
2020	Salvatore et al., 2020	MasterRoc MP 325	0.429	3; 5; 10	0.9 to 3.1	0.005 to 0.018	sand	Permeation from base (until immersion complete)	Vane test TXCID CTXCIU

666 * : As compacted/poured soil porosity

667

668 *Table 2 Physical and chemical properties of the base materials*

669

	Holcim sand	Carbonate silt	Sand with 10% carbonate silt	Metakaolin powder	Colloidal Silica
Quartz content (w/w, %)	92.1	-	82.9	55	40
$CaCO_3$content (w/w, %)	-	98.2	9.8	-	-
pH value	6.69	9.90	-	6	7-9
Maximum grain size, d_{100} (mm)	0.710	0.161	0.710	0.080*	-
Mean grain size, d_{50} (mm)	0.450	0.033	0.450	0.010-0.015	$1.5 \cdot 10^{-5}$ **
Grain size, d_{10} (mm)	0.336	0.003	0.172	-	-
Coefficient of uniformity	1.4	-	1.8	-	-
Grains fraction < 2 μm (%)	-	8.0	0.8	100	100
Density of solids, ρ_s (Mg/m^3)	2.65	2.71	2.66	2.40	2.11 **
Hygroscopic w/c (%) at RH=50%	<0.3	0.1	<0.3	-	-
Bulk density as poured (Mg/m^3)	1.34	1.10	1.47	-	-
Void ratio as poured	0.825	0.464	0.584		-
Hydraulic conductivity as poured, k_w (m/s)	$7.67 \cdot 10^{-4}$	-	$2.85 \cdot 10^{-4}$		-
Maximum void ratio, e_{max}	0.982	-	-	-	-
Minimum void ratio, e_{min}	0.532	-	-	-	-

* d_{95}

** Wong et al., 2018

670

671

672

673

674

675

676 *Table 3 Characteristics of the binders.*

		Geopolymer (MK)	Colloidal Silica (CS)
Binder	Precursor material	Metakaolin powder	Aqueous dispersion of silica
	Activator (*) / Accelerator (**)	Potassium silicate (K_2SiO_4) (*)	De-aired water + 12% added to volume of NaCl (10% w/w) (**)
Precursor : activator / accelerator (V/V)		1:1	8.3:1
Other fractions		De-aired water	-
Water/binder (w/w)		1:2	-
% of void's volume filling		40% - 100%	100%
Binder-soil mixing technique		Hand-mixing	Low-pressure permeation
Curing conditions		50% RH / Under water (20°C)	50% RH (20°C)
Base soils		S / SO	S / SO
Density at slurry/liquid state (Mg/m^3)		1.37	1.30

677

678

679 *Table 4 Material proportions in the mixtures.*

			Geopolymer (MK)					Colloidal Silica (CS)				
Size	Soil	F_0 = V_{fluid}/V_{pores} (%)	Geopolymer slurry/dry soil (w/w)	Metakaolin powder/dry soil (w/w)	C_{iv} = $V_{MKpowder}/V_{tot}$ (-)	η / C_{iv} (-)	w/c_0 (-)	Colloidal Silica slurry*/dry soil (w/w)	Silica / dry soil (w/w)	C_{iv} = $V_{silicar}/V_{tot}$ (-)	η /C_{iv} (-)	w/c_0 (-)
UC	S	100	0.43	0.14	0.086	5.3	1	0.40	0.14	0.075	6.0	1.8
TX	S	100	0.43	0.14	0.086	5.3	1	0.40	0.14	0.075	6.0	1.8
UC	SO	100	0.27	0.09	0.061	5.3	1	0.28	0.09	0.053	6.0	1.8
TX	SO	100	0.27	0.09	0.061	5.3	1	0.28	0.09	0.053	6.0	1.8
TX	S	40	0.17	0.06	0.034	13.1	1	n.a.	n.a	n.a.	n.a.	n.a.
TX	SO	40	0.11	0.04	0.024	13.1	1	n.a.	n.a.	n.a.	n.a.	n.a.
* aqueous dispersion + accelerant												

680

681 *Table 5 Overview of the tests performed and treated soils tested. Number of curing days in parenthesis*

	Unconfined compression tests (UCS)	Consolidated-Undrained Static Triaxial Tests (TXCIU)	Consolidated-Undrained Cyclic Triaxial Tests (CTXU)
S		X	X
SO		X	X
SMK(100)D	X (3,7,28)	X (3,7,28)	
SMK(100)W	X (3,7,28)		
SMK(40)D		X (3,7,28)	
SMK(40)W			X (7)
SOMK(100)D	X (3,7,28)	X (3,7,28)	
SOMK(40)D		X (3,7,28)	
SOMK(40)W			X (7)
SCS(100)D	X (1,7,28)	X (3,7,28)	X (7)
SOCS(100)D	X (1,7,28)	X (3,7,28)	X (7)

682

683

684 *Table 6 Density of grains in the mixture, dry density, water content and void ratio of CS-treated samples.*

	ρ_s* (Mg/m^3)	ρ_d (Mg/m^3)	w (%)	as-treated void ratio, *e* (-)
SCS(100)D28	2.47	1.70	0.12	0.453
SOCS(100)D28	2.49	1.72	0.13	0.448

685 ρ_s* calculated as weighed average of the constituent fractions

686

687 *Table 7 Summary of mixture characteristics from the FA geopolymer studies of Rios et al. (2017a;*
688 *2017b)*

Author	Sample ID	As poured/compacted porosity, η (-)	Binder powder/dry soil (w/w) %	C_{iv} (-)	η / C_{iv} (-)
Rios et al. (2017a)	n.a.	0.248	20	0.150	1.65
Rios et al. (2017b)	M1	0.298	18	0.124	2.41
	M2	0.342	25	0.164	2.08
	M3	0.382	33	0.206	1.86

689

690

691 *Table 8 Strength parameters obtained by the different treatments.*

	SMK(100)	SMK(40)	SOMK(100)	SOMK(40)	SCS(100)	SOCS(100)	S	SO
c' (kPa)	225	20	310	84	26	26	0	0
φ' (°)	48	48	48	48	41	41	38	38

692

693

FIGURES

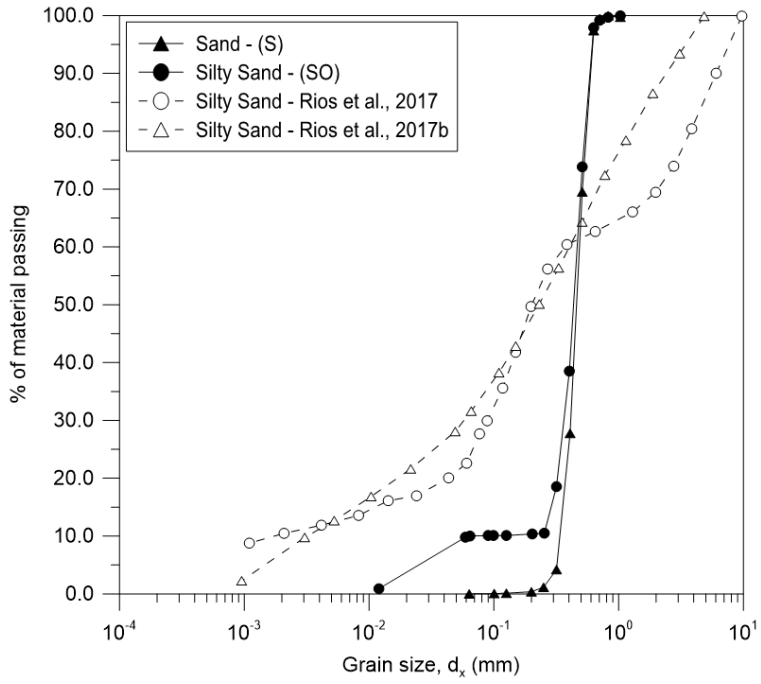

Figure 1 Grain size distributions of base soils

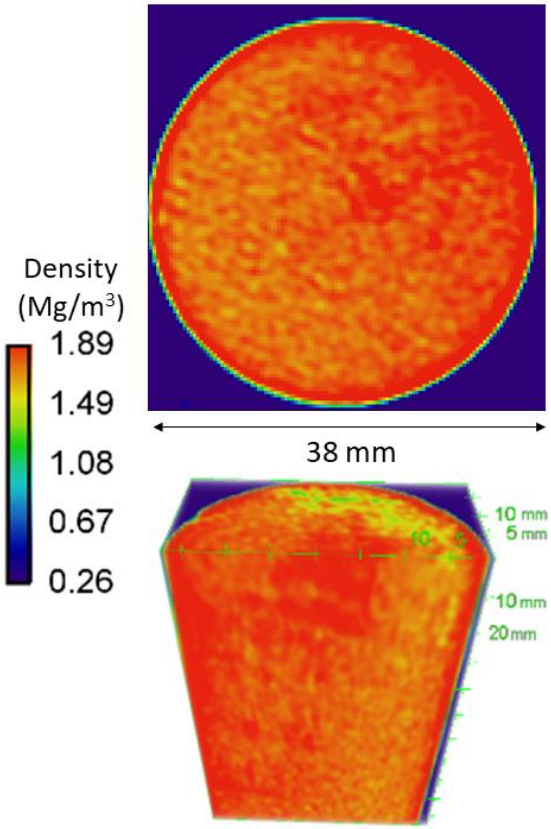

699

700 *Figure 2 CT scan of CS injected TX specimen of silty sand with density map*

701

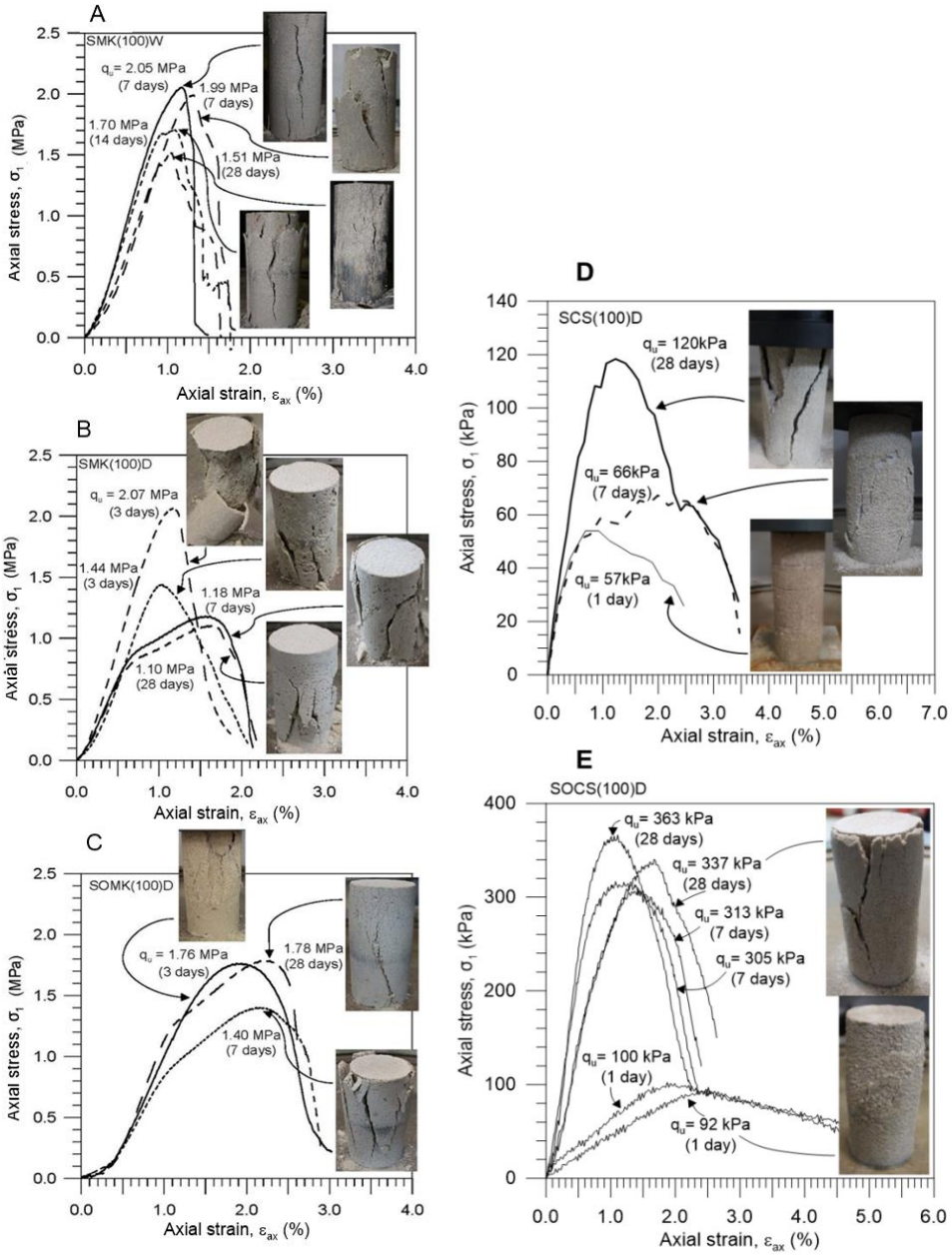

Figure 3 UCS tests results and images of some broken samples. A) SMK cured at relative humidity RH = 50%, B) SMK cured in submerged conditions, C) SOMK cured at relative humidity RH = 50%, D) SCS cured at relative humidity RH = 50%and E) SOCS cured at relative humidity RH = 50%.

.

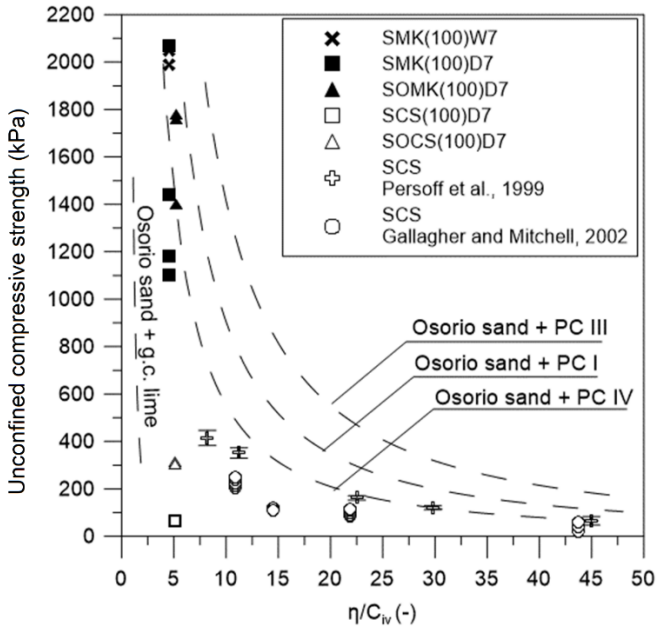

(a)

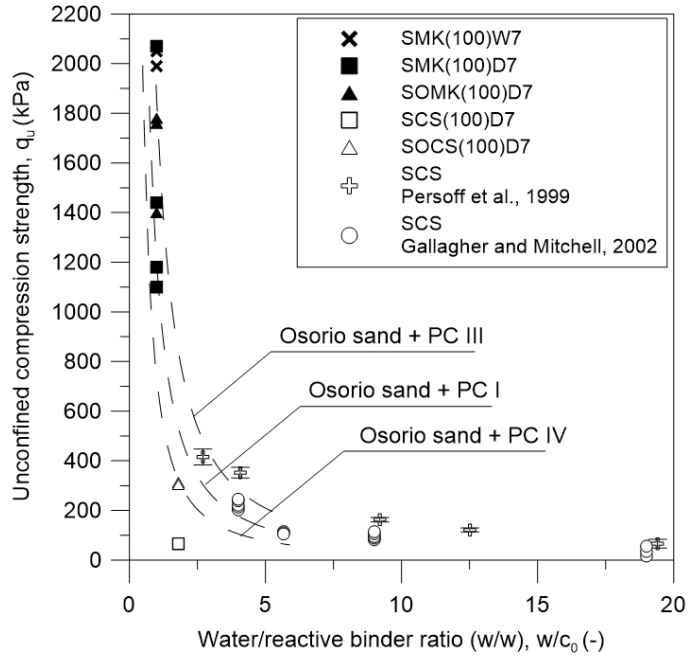

(b)

Figure 4 Strength vs mixture ratios for the specimens expressed as (a) porosity / volumetric binder ratio (b) water content / ponderal binder ratio. Comparisons with literature results on sand treated with Portland Cement (Consoli et al., 2011; 2016) sand with waste glass-carbide lime (Consoli et al., 2020). All results for specimens cured 7 days (except Gallagher and Mitchell, 4 to 56 days).

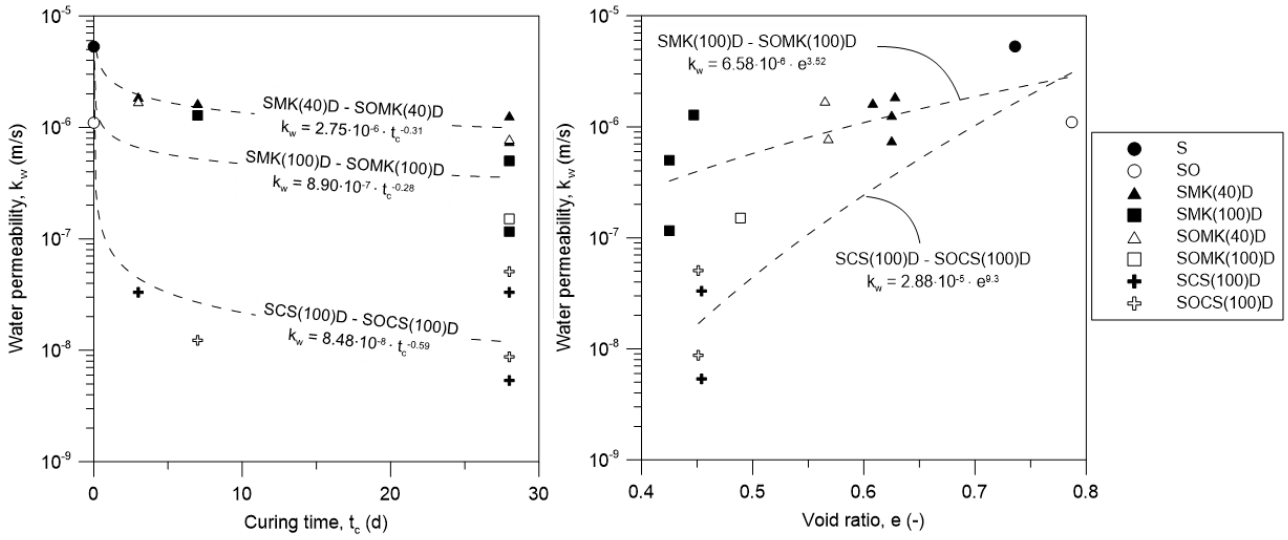

Figure 5 evolution of the saturated water permeability with: a) curing time, b) as-cured void ratio.

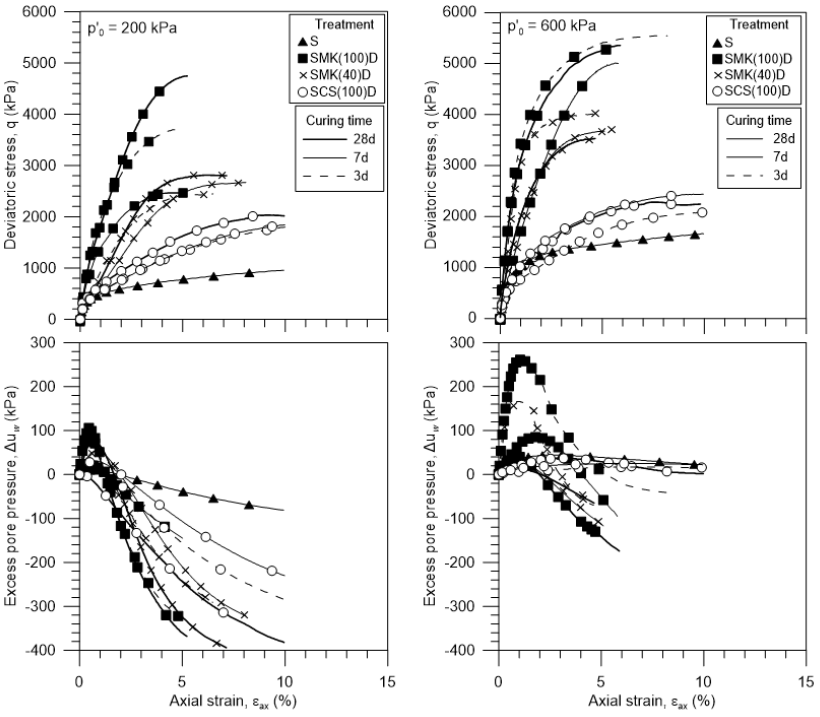

Figure 6 Deviatoric stress and excess pore water pressure vs axial strain for consolidated undrained triaxial compressions on specimens of sand with and without binders. Results after consolidation to: a) p'_0 = 200 kPa, b) p'_0 = 600 kPa.

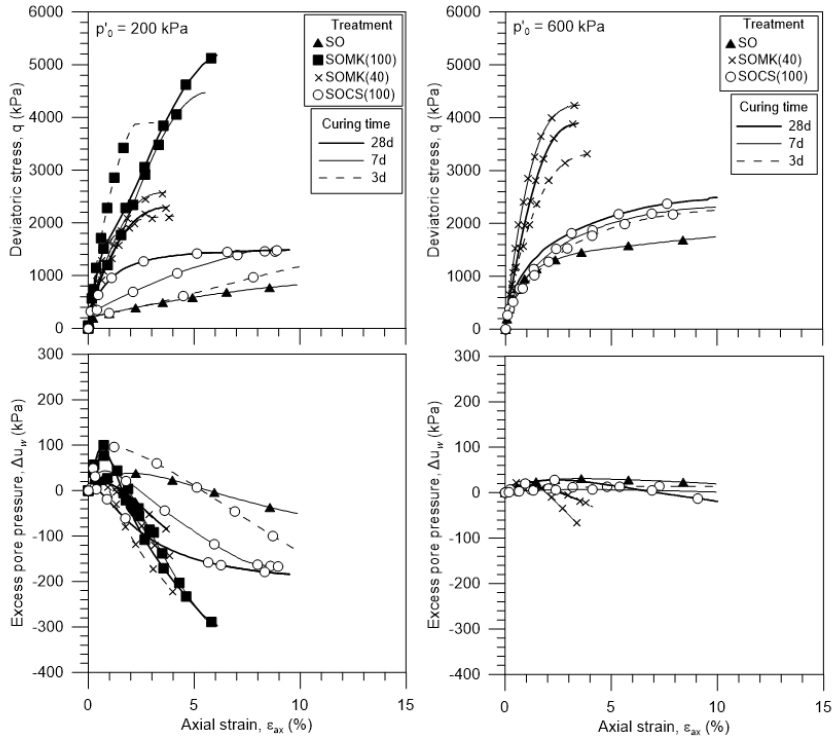

722

723 *Figure 7 Deviatoric stress and excess pore water pressure vs axial strain for consolidated undrained*
724 *triaxial compressions on specimens of sandy silt with and without binders. Different consolidation*
725 *stresses: a) p'0 = 200 kPa, b) p'0 = 600 kPa*

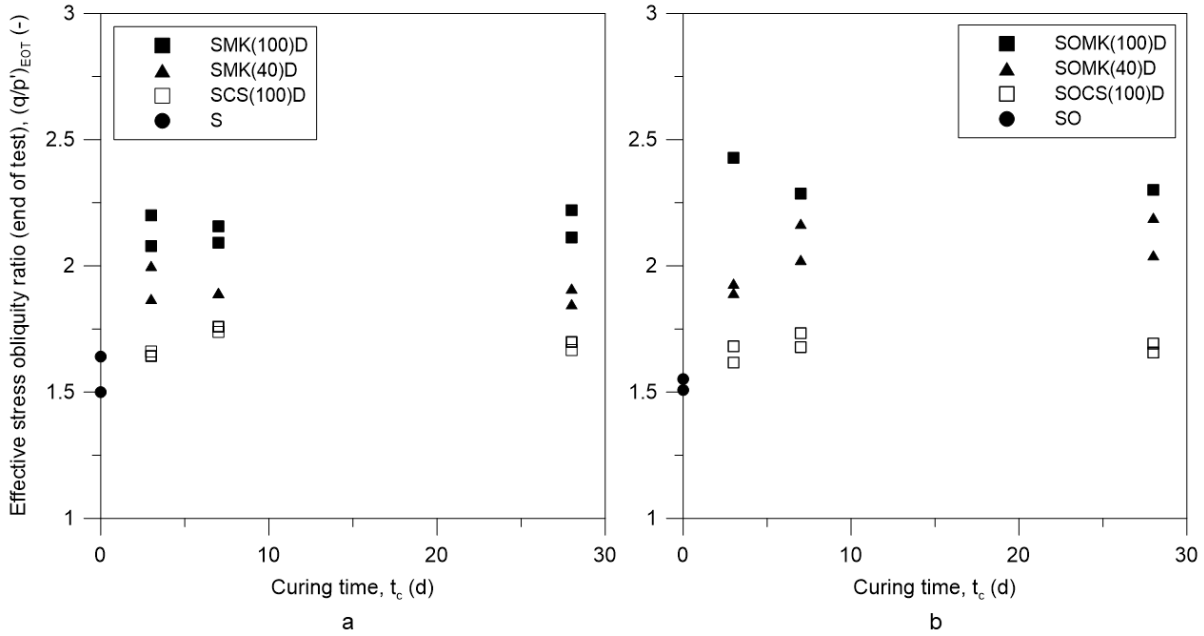

726

727 *Figure 8 Mobilised strength at failure in TXCIU tests for (a) sand with and without binders (b) silty -sand*
728 *with and without binders*

729

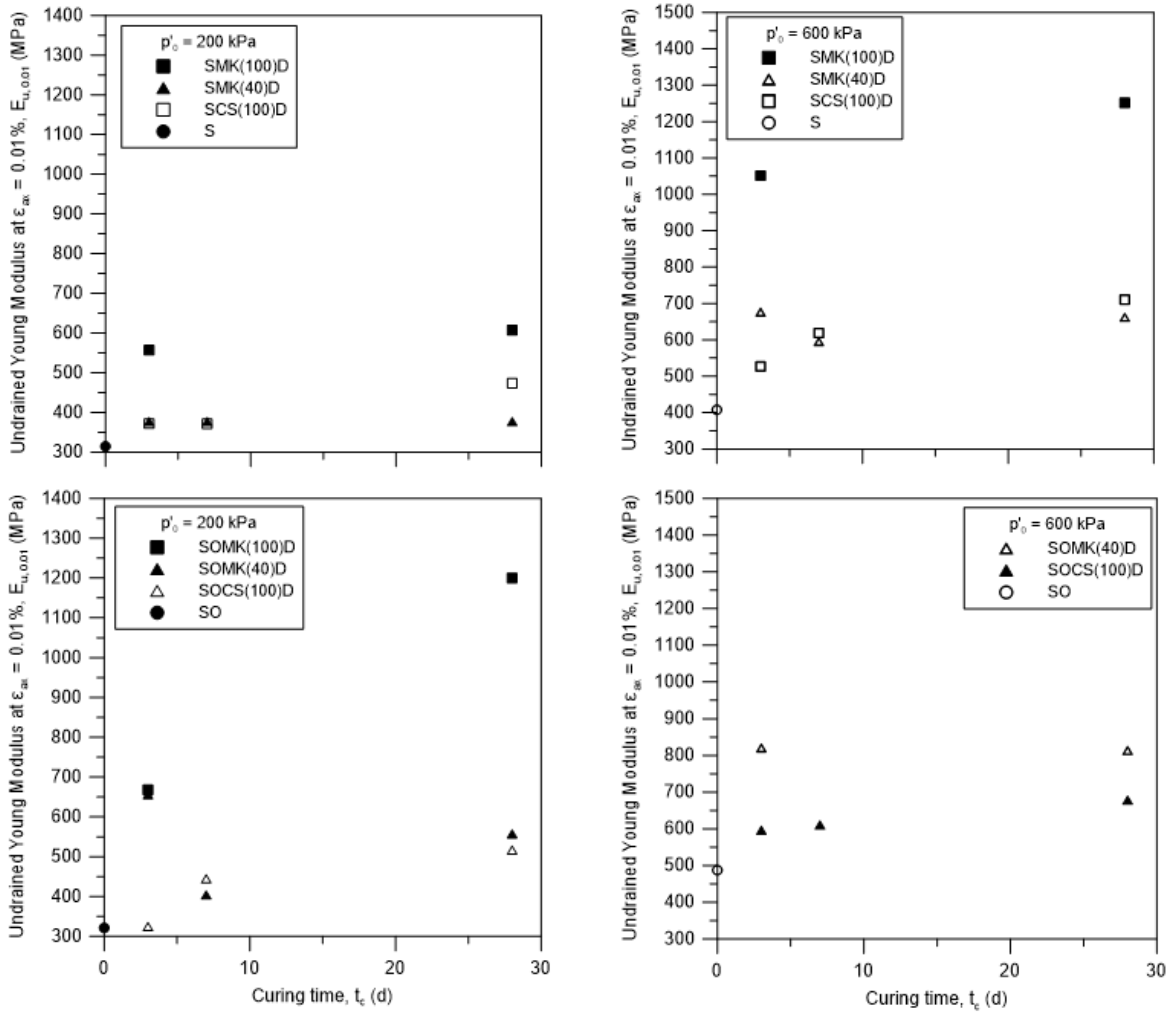

730

731 *Figure 9 TXCIU Secant undrained Young Modulus at ε_{ax} = 0.01%*

732

733

734

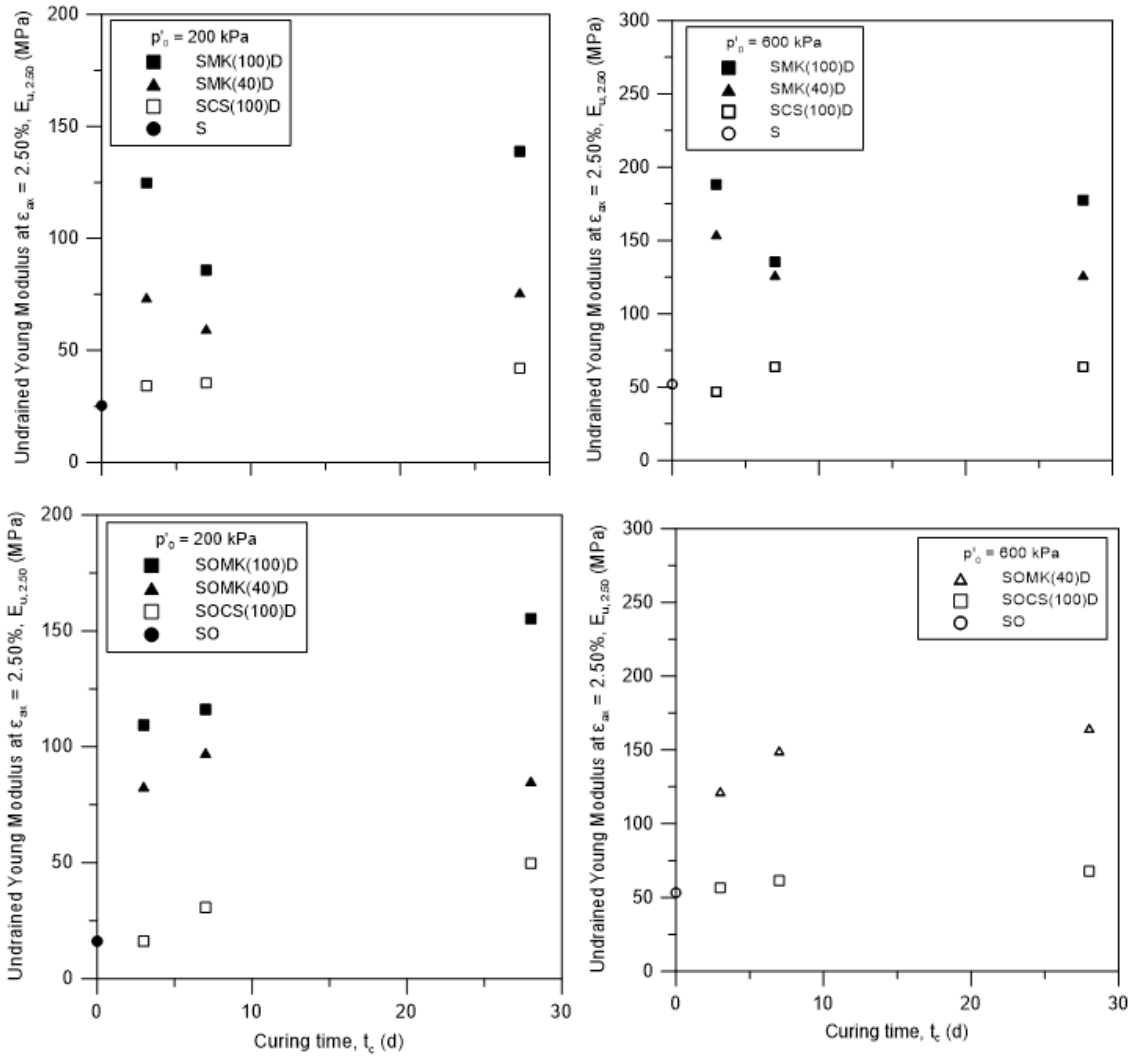

735

736 *Figure 10 TXCIU Secant undrained Young Modulus at ε_{ax} = 2.50%*

737

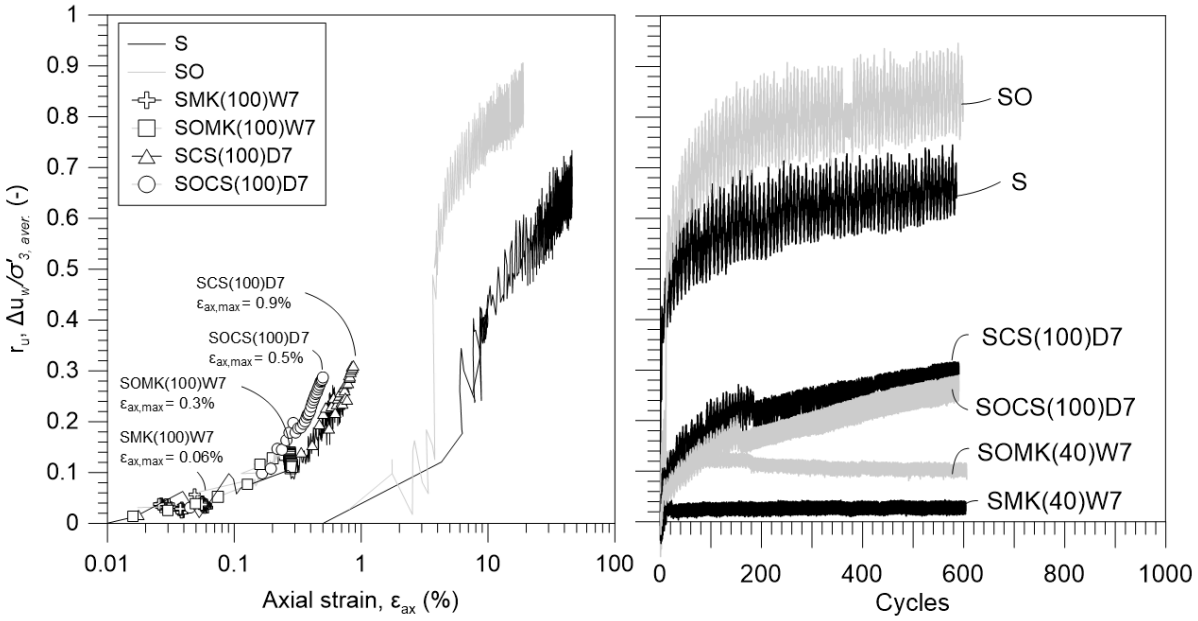

738

739 *Figure 11 Evolution of the normalized excess pore water pressure as a function of axial strains (left) and*
740 *number of applied cycles (right).*

741

742

743

744

745

746

747

748

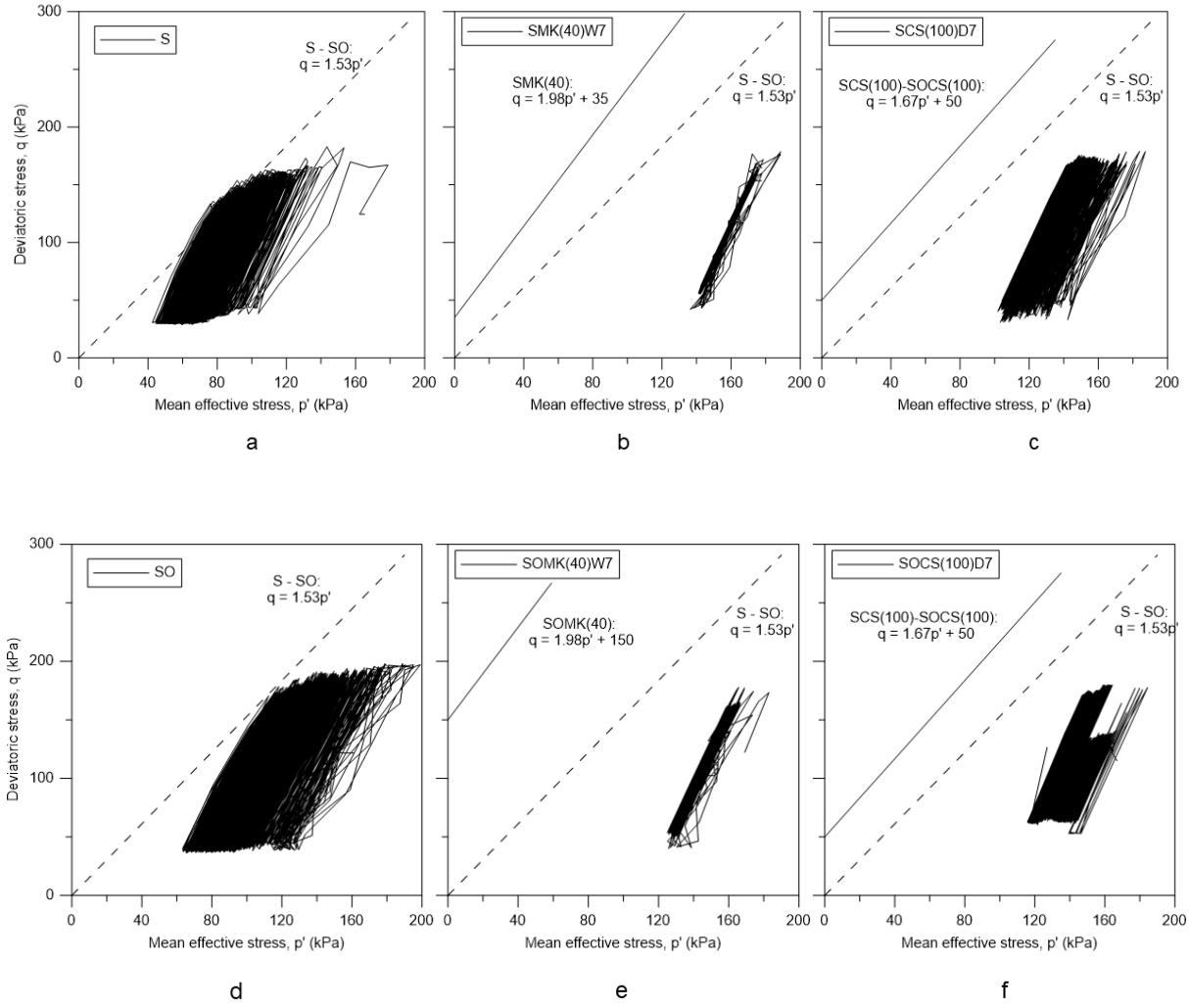

Figure 12 Evolution of the stress state in CTXC tests and comparisons with failure envelopes obtained by TXC.

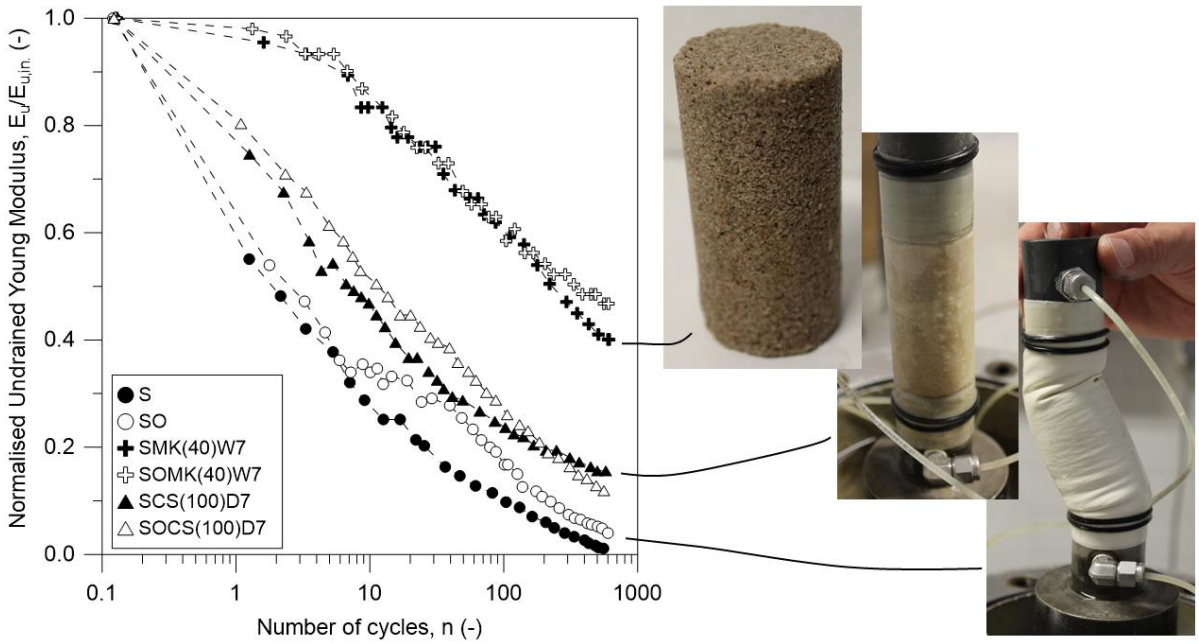

754

755 *Figure 13 Cyclic stiffness degradation in the untreated and treated specimens, jointly with some samples*
756 *at the end of test.*

757

758

759

760

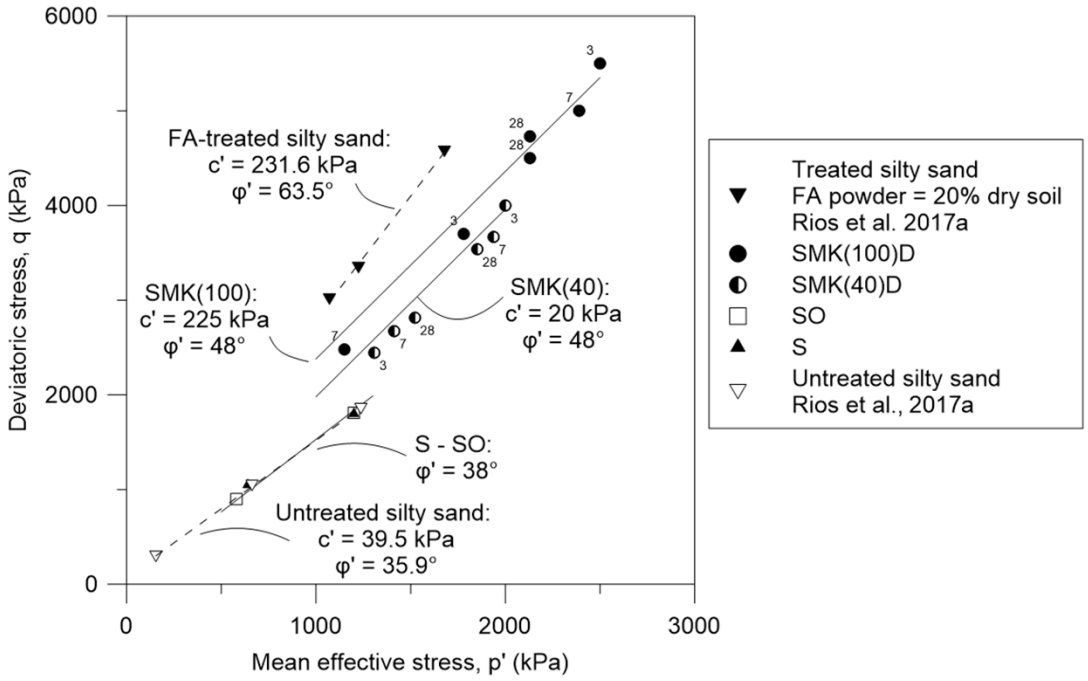

761

762 *Figure 14 Peak strength envelopes for treated and untreated soils. Treated soils include the silty sand*
763 *treated with a Fly-ash (FA)-based geopolymer (Rios et al., 2017a) and Holcim sand treated with a MK-*
764 *based geopolymer (this study)*

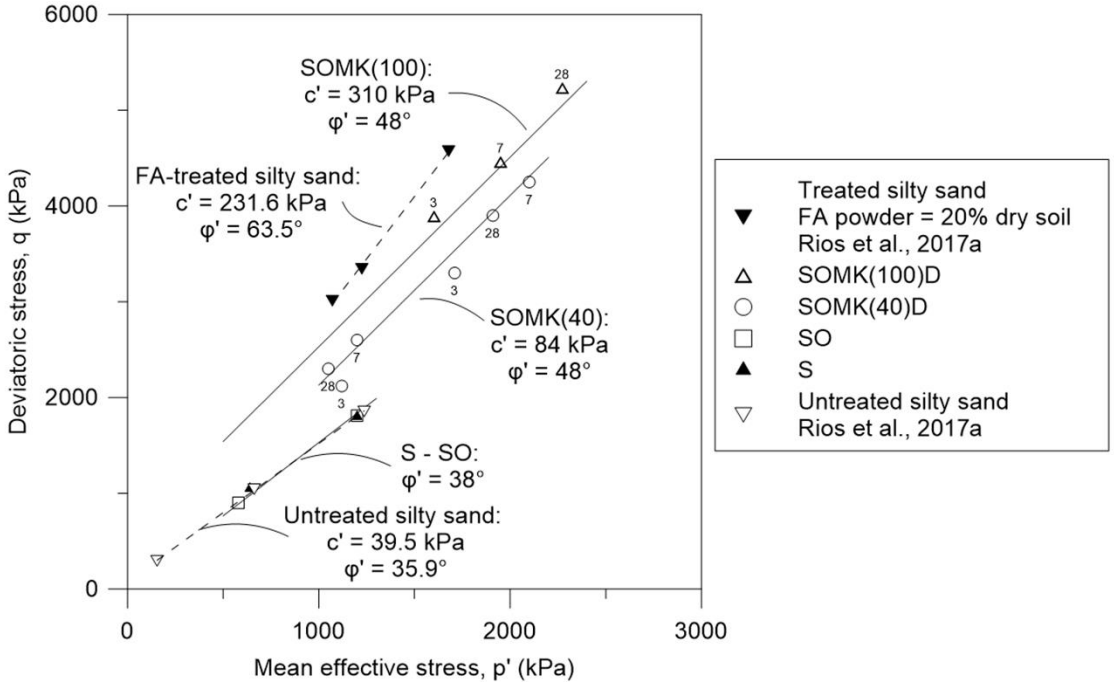

765

766 *Figure 15 Peak strength envelopes for treated and untreated soils. Treated soils include the silty sand*
767 *treated with a Fly-ash (FA)-based geopolymer (Rios et al., 2017a) and Holcim sand treated with a MK-*
768 *based geopolymer (this study)*

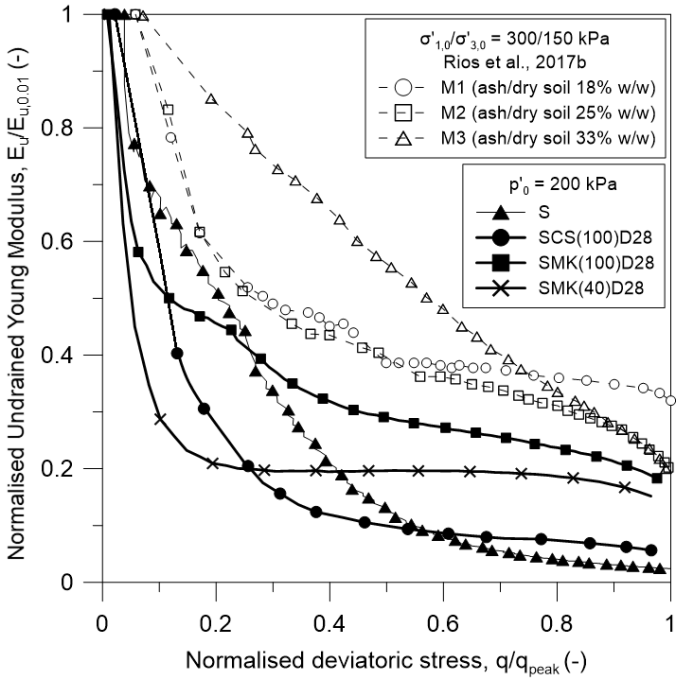

769

770 *Figure 16 Secant stiffness degradation during monotonic triaxial shearing for different geopolymer im-*
771 *proved soils*

772

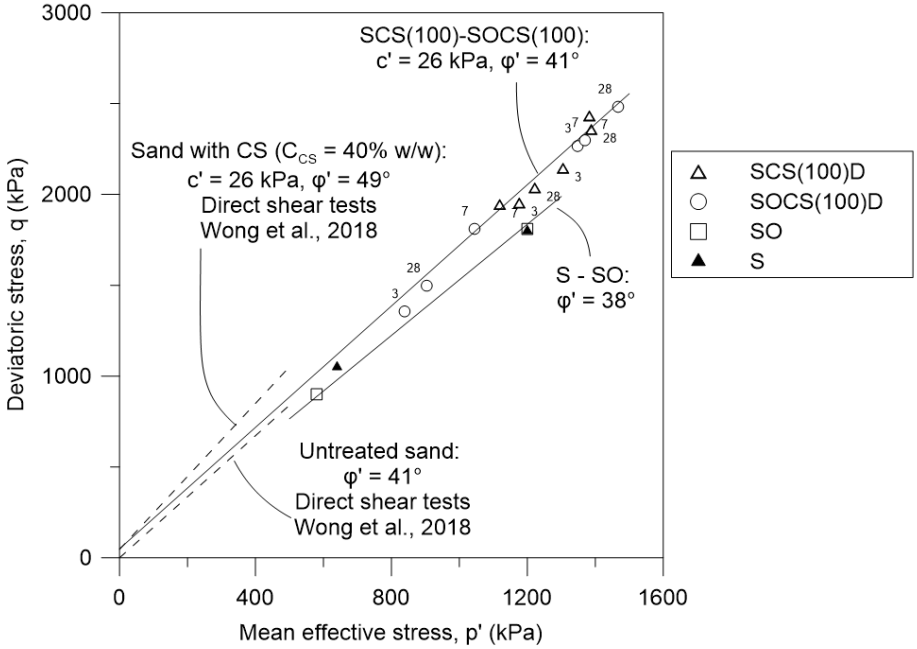

773

774 *Figure 17 CS treated sands (this study+literature). Comparisons between TXC and Direct Shear tests*
775 *at low vertical stresses (σ_1 < 300 kPa) on samples treated with the same CS product (MP 320, silica*
776 *concentration in the solution C_{CS} = 40%).*

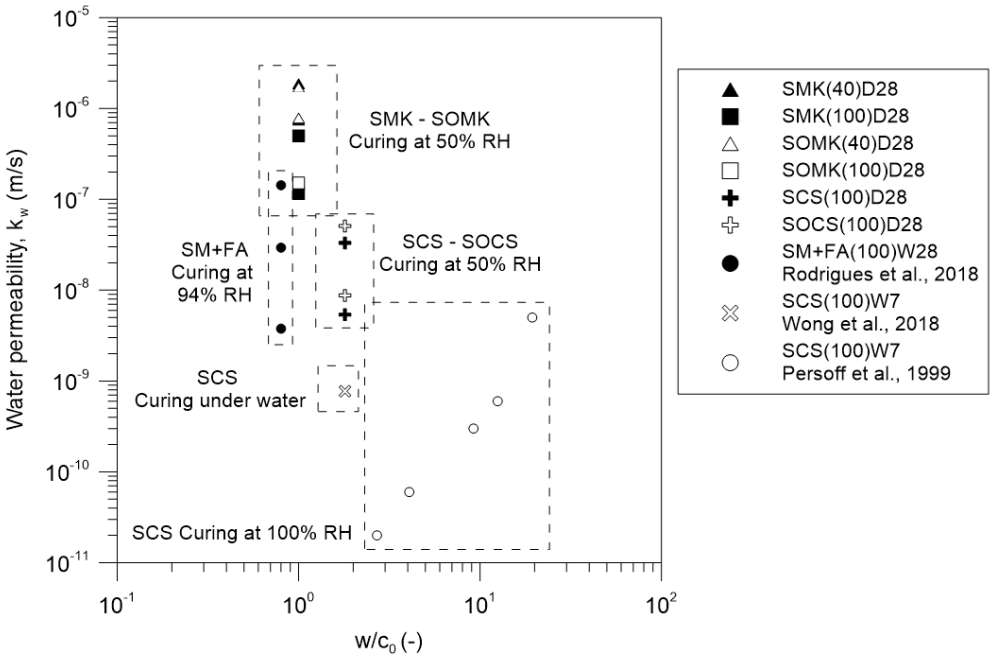

777

778 *Figure 18 Permeability vs water content / ponderal binder ratio for the materials tested in this study and*
779 *literature values for other CS and fly ash geopolymer treatments.*

780

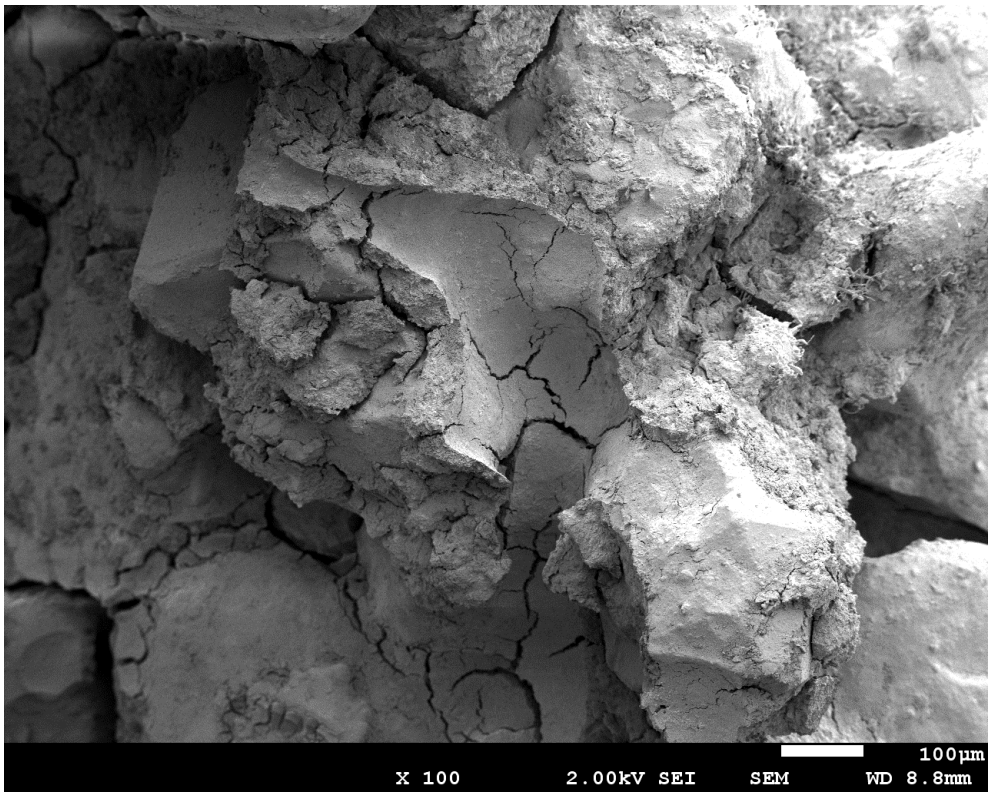

781

782 *Figure 19 FESEM image of specimen SMKD(40). Sand grains are bound by cracked geopolymer*
783 *bridges*

784